Savannah River National Laboratory®

A U.S. DEPARTMENT OF ENERGY NATIONAL LAB • SAVANNAH RIVER SITE • AIKEN, SC • USA

Mini-Canister Radiolysis Testing of ASNF Materials and Surrogates

Anna L. d'Entremont, Christopher G. Verst

October 31, 2024

SRNL-STI-2024-00359, Revision 0

srnl.gov

DISCLAIMER

Printed in the United States of America

Prepared for
U.S. Department of Energy

SRNL-STI-2024-00359
Revision 0

Keywords: Radiolysis, aluminum-clad spent nuclear fuel, dry storage, drying

Retention: *Varies (Track number is applicable)*

Mini-Canister Radiolysis Testing of ASNF Materials and Surrogates

Anna L. d'Entremont
Christopher G. Verst

October 31, 2024

Savannah River National Laboratory is operated by Battelle Savannah River Alliance for the U.S. Department of Energy under Contract No. 89303321CEM000080.

REVIEWS AND APPROVALS

AUTHORS:

ANNA D'ENTREMONT (Affiliate)
Digitally signed by ANNA D'ENTREMONT (Affiliate)
Date: 2024.10.31 15:48:01 -04'00'

Anna L. d'Entremont, Materials Science & Disposition Date

Digitally signed by CHRISTOPHER VERST (Affiliate)
Date: 2024.11.04 12:14:34 -05'00'

Christopher G. Verst, Materials Science & Disposition Date

TECHNICAL REVIEWERS:

CHARLES CRAWFORD (Affiliate)
Digitally signed by CHARLES CRAWFORD (Affiliate)
Date: 2024.11.04 12:22:46 -05'00'

Charles L. Crawford, Glass, Cement, & Ceramic Science Date

APPROVAL:

MORGANA WHITESIDE (Affiliate)
Digitally signed by MORGANA WHITESIDE (Affiliate)
Date: 2024.11.04 12:30:02 -05'00'

Morgana T. Whiteside, Materials Science & Disposition/Manager Date

JOSEPH MANNA (Affiliate)
Digitally signed by JOSEPH MANNA (Affiliate)
Date: 2024.11.04 17:17:42 -05'00'

Joseph Manna, Materials Technology & Energy Sciences/Division Director Date

PREFACE

Radiolysis of residual water within spent nuclear fuel (SNF) dry storage canisters can alter the headspace gas conditions, with the potential for build-up of hydrogen gas (H_2) in sealed canisters. The residual water can be in the form of free water (vapor or liquid), physisorbed water on the surfaces of SNF and canister internals, and chemisorbed/chemically bound water incorporated into compounds such as (oxy)hydroxides on the SNF and canister internals. Each of the sources of residual water can undergo radiolysis reactions whereby it breaks down under the attendant radiation of the SNF leading to generation of stable hydrogen (H_2) that collects in the headspace gas.

Aluminum-clad spent nuclear fuel (ASNF) in particular can hold significant amounts of chemisorbed water in the form of aluminum (oxy)hydroxide layers that form on the surface of the cladding under exposure to water during use and storage and are not readily removed at low (<100°C) drying temperatures. As a result, quantification of radiolytic gas generation from materials with surface conditions representative of ASNF materials is important to establish expected H_2 generation rates and overall yields so that the behavior of ASNF in dry storage can be reliably evaluated/predicted.

The work described in this report is the summary and status of radiolysis experiments for ASNF using the SRNL mini-canister testing system. The investigation involves measuring the H_2 gas buildup in an initial cover gas of dry helium from materials with an aluminum substrate and a film of aluminum (oxy)hydroxide. The separate experimental campaigns involved application of different drying treatments (vacuum and/or heating steps, plus a nominally undried condition) to plates of an aluminum cladding alloy corroded to produce a layer of bayerite ($Al(OH)_3$); these samples were gamma-irradiated using a Co-60 irradiator, and the gas was sampled at intervals during irradiation to monitor the H_2 gas evolution. A separate campaign using a reactor-exposed and basin-stored end fitting cut from an ASNF fuel element with a service-formed (oxy)hydroxide layer is also reported. The results of this testing are compared to results of previous radiolysis investigations in glass ampoules to assess implications for ASNF dry storage and modeling thereof.

The body of work to investigate the radiolysis of ASNF in dry storage conditions has been done in collaboration with Idaho National Laboratory (INL), with sponsorship by the DOE-EM Office of Technology Development.

EXECUTIVE SUMMARY

An experimental irradiation campaign to investigate radiolysis behavior of ASNF was conducted using in-situ gas monitoring of small, sealed stainless-steel vessels (mini-canisters) containing aluminum samples with adherent (oxy)hydroxide films under helium backfill. The samples were irradiated with gamma radiation from a Co-60 irradiator. The samples tested included aluminum plate assemblies with lab-grown (oxy)hydroxides as surrogates for fuel as well as an end cropping from an actual ASNF assembly retrieved from long-term wet storage. These experiments enabled investigation of the impacts of various fuel drying approaches on the radiolytic generation rate and measurement of the H_2 yield associated with a reactor-exposed sample with reactor-formed (oxy)hydroxide. The resulting data can be incorporated into model development for ASNF in dry storage.

This report presents the cumulative results from four surrogate assemblies tested after application of different preparation (drying) conditions as well as the ASNF cropping; some post-irradiation testing was included. The mini-canister results are compared to data from related experimental campaigns that also tested the impact of drying conditions using samples irradiated in glass ampoules and discusses implications of the combined data.

The gas samples withdrawn from the canisters were characterized to measure the amount of H_2, N_2, and O_2. Net generation was observed only for H_2, with no evidence of radiolytic O_2 generation, consistent with previous radiolysis testing. (N_2 generation was not expected; it was monitored as an indicator for residual air or leaks.) The H_2 generation rates were largest at the beginning of irradiation and tended to decrease with increasing dose.

The mini-canister results showed a large reduction in H_2 generation for samples subjected to heated drying (at 150°C or 220°C) prior to irradiation, compared to a nominally undried/air-dried sample. By contrast, an extended (12-h), unheated vacuum step appeared to provide minimal reduction in H_2 generation rate over the (low-dose) range where data was collected. The reduction in H_2 yield was hypothesized to result largely from removal of physisorbed water, since there was little difference in yield between the two heated drying conditions, despite only the 220°C condition being expected to remove chemisorbed water. Drying tests for samples in glass ampoules have provided some conflicting and/or ambiguous data: Some ampoule tests showed larger impacts from unheated vacuum drying than were observed in the mini-canisters and other tests showed minimal differences between vacuum and heated drying. The reasons behind these apparent discrepancies are not yet clear.

Although evidence points to physisorbed water accounting for much of the initial H_2 generation, the amount of chemisorbed water bound in the aluminum (oxy)hydroxide films is expected to be a much larger reservoir of water and hydrogen than the physisorbed water, and heated drying to temperatures high enough to dehydrate aluminum trihydroxide ($Al(OH)_3$) remains the only clear path to reducing the chemisorbed inventory.

TABLE OF CONTENTS

LIST OF TABLES

LIST OF FIGURES

LIST OF ABBREVIATIONS

ASNF	Aluminum-clad spent nuclear fuel
DOE	U.S. Department of Energy
FHD	Forced helium dehydration
GC	Gas chromatograph
INL	Idaho National Laboratory
MURR	Missouri University Research Reactor
SEM	Scanning electron microscopy
SNF	Spent nuclear fuel
SRNL	Savannah River National Laboratory
SRS	Savannah River Site
XRD	X-ray diffraction

1.0 Introduction

The U.S. Department of Energy (DOE) manages a large inventory of aluminum-clad spent nuclear fuel (ASNF) from U.S. High Performance Research Reactors and also from some foreign research reactors; this ASNF is in interim storage pending ultimate disposition. The current disposition path for DOE-owned ASNF is chemical dissolution and processing, but the single USA processing facility (Savannah River Site's H-canyon) is currently scheduled for shutdown, so an alternative disposition strategy is needed for future ASNF that will continue to be generated. Dry storage in sealed canisters is an established long-term storage approach for commercial (Zr-clad) spent nuclear fuel (SNF) and is a potential pathway for interim storage and/or disposition of ASNF. Interim storage must be suitable for an extended storage duration (>50 years) since no repository currently exists.

Although dry storage canisters and their contents are subjected to drying processes prior to sealing, some small amount of residual water will remain trapped in the canisters, whether in the form of free water, physisorbed water, or chemisorbed/chemically bound water in compounds such as (oxy)hydroxides, and radiolysis of the residual water can lead to build-up of hydrogen gas. ASNF in particular can hold significant amounts of chemisorbed water in the form of aluminum (oxy)hydroxide layers that form on the outside of the cladding and are not readily removed at low (<100°C) drying temperatures. Quantification of radiolytic gas generation from materials with surface conditions representative of ASNF materials and under canister-analogous conditions is important for establishing expected H_2 generation rates/yields and enabling predictions of the conditions of ASNF in dry storage canisters.

For this purpose, an experimental irradiation campaign was conducted using in-situ gas sampling of small, sealed stainless-steel vessels (mini-canisters) containing aluminum samples under helium backfill and subjected to gamma irradiation. The mini-canisters feature a gas sampling line through the lid that allows repeated sampling of the gas space without opening the canister. The samples tested included aluminum plate assemblies with lab-grown (oxy)hydroxides as fuel surrogates as well as an end cropping from an actual ASNF assembly retrieved from long-term wet storage. These experiments enabled investigation of the impacts of various fuel drying approaches on the radiolytic generation rate and measurement of the H_2 yield associated with a reactor-exposed sample with reactor-formed (oxy)hydroxide. The studies provide empirical data for developing predictive models of ASNF in dry storage.

The gas sampling approach allows tracking of the H_2 generation rate of an individual sample and preparation condition from its early H_2 release through its longer-term behavior, in contrast to ampoule-based approaches that provide only a single data point per sample/ampoule at the end of its test period. This test campaign provides data on how the H_2 generation of an individual sample evolves over time, which is used in the development of multi-physics ASNF canister models and allows investigation of the impact of drying processes on radiolytic H_2 yield. A similar gas sampling approach will be used in a planned full-scale pilot canister as verification and validation of the dry storage safety basis for ASNF [1].

This report presents the results of four surrogate assemblies tested under different preparation (drying) conditions as well as the ASNF cropping and results of some post-irradiation testing. It discusses implications of the data, comparisons to the results of other radiolysis tests, and their application to models.

2.0 Experimental Setup and Procedure

2.1 Mini-canisters

The mini-canisters were steel vacuum vessels with an inner diameter of 2.83 in (7.19 cm) and height of 7.06 in (17.9 cm). They were sealed with a bolted closure featuring a knife-edged conflat seal with copper gaskets to provide leak tightness up to ultra-high vacuum, and the lid features a Swagelok threaded connection to a 6-ft long steel capillary line for filling or extracting gas while the lid is sealed. The mini-

canisters are designed to be bench-scale surrogates for dry storage canisters, i.e., a stainless-steel vessel backfilled with helium, to facilitate irradiation of the samples in a canister-analogous environment.

During irradiation, small gas samples are periodically withdrawn from the vessel through the sampling line to measure the gas pressure and the concentrations of H_2, O_2, and N_2. H_2 is the primary expected gaseous product of the radiolysis; O_2 is a potential product of radiolysis if the oxygen does not remain in the solid or react with other materials in the canister, and N_2 is not expected to be produced by any reaction in the sealed canister but serves as an indicator of residual air or air ingress into the canister.

2.2 Surrogate samples

Four surrogate plate assemblies were used for mini-canister testing. Each consisted of 17 individual, 0.050-in (1.3-mm) thick plates of aluminum 6061-T6 alloy, which were bolted together with aluminum hardware and separated by aluminum washers providing a 2-mm gap between plates. The plate height and widths were selected to conform closely to the cylindrical interior of the mini-canisters in order to maximize the plate surface area in the test (dimensions given in Appendix A, Table 7-1). The resulting aluminum surface area was roughly 3800 cm^2.

The four assemblies were used to test four different drying conditions. They are briefly summarized as follows in order of increasing drying (more detail on the preparation conditions is provided in subsequent sections):

- *As-Corroded No-Vacuum:* Air-dried (for >16 h, no extended vacuum or heating) and exposed only to seven, brief (~5-s) vacuum steps alternating with helium purges to eliminate residual air from the canister; expected to represent a nominally undried surface condition.
- *As-Corroded Vacuum-Only:* Vacuum-dried (for 12 h) without heating; expected to remove free and some physisorbed water without altering the (oxy)hydroxide film.
- *150°C As-Dried:* Moderate-temperature heated drying at 150°C (for 4 h), below the (220°C) temperature threshold for bayerite thermal decomposition; expected to remove free and most physisorbed water without significantly altering the (oxy)hydroxide film.
- *220°C As-Dried:* High-temperature heated drying at 220°C (for 4 h), the temperature threshold for bayerite thermal decomposition; expected to remove free, physisorbed, and some chemisorbed water.

The As-Corroded Vacuum-Only and 220°C As-Dried were the initial conditions investigated (originally designated simply “As-Corroded” and “As-Dried”) [2, 3], while the 150°C As-Dried [4] and As-Corroded No-Vacuum conditions [5] were added later to clarify behaviors.

All four plate assemblies were corroded in room-temperature distilled water to form a bayerite film prior to testing. Immediately prior to immersion, the plates were polished to a 600-grit finish and rinsed with distilled water. The corrosion durations and associated mass gains are provided in Table 2-1. The As-Corroded Vacuum-Only and 220°C As-Dried assemblies each had a sample removed from one plate of the assembly prior to being sealed into their mini-canisters; these samples were used for characterization of the initial (oxy)hydroxide layers of the corresponding assemblies, and their removal accounts for the reduced

mass of these two assemblies in Table 2-1. The 220°C As-Dried characterization sample was dried alongside the corresponding canister so that the impacts of drying on the (oxy)hydroxide could be assessed.

Table 2-1. Corrosion data for the surrogate plate assemblies.

Name	Days immersed	Uncorroded mass (g)	Corroded mass (g)	Corrosion mass gain (g)	Mass gain (%)
As-Corroded No-Vacuum	33	633.1	637.4	4.3	0.68%
As-Corroded Vacuum-Only	41	611.2	616.7	5.5	0.90%
150°C As-Dried	33	636.1	640.4	4.3	0.68%
220°C As-Dried	36	611.5	616.8	5.3	0.87%

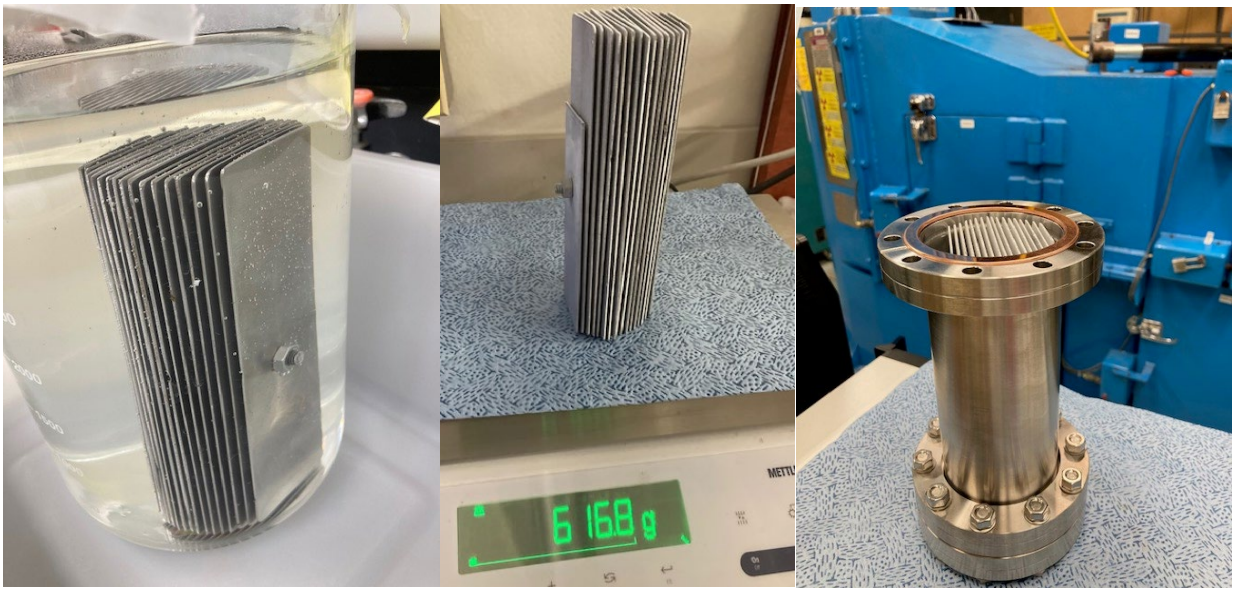

Figure 2-1. 220°C As-Dried plate assembly (left) during and (center) after corrosion in room-temperature water and (right) loaded into its canister prior to closure and drying.

The later surrogate assemblies reused the same two mini-canister vessels from the original tests. The canister originally used for the As-Corroded Vacuum-Only sample was subsequently used for the 150°C As-Dried test, and the canister originally used for the 220°C As-Dried sample was reused for the As-Corroded No-Vacuum test.

2.3 Missouri University Research Reactor (MURR) sample

The reactor-exposed sample was a cropping from the end of a Missouri University Research Reactor (MURR) fuel element made of aluminum alloy 6061-T6; the original intact cropping is shown in Figure 2-2 (left). The service history of the individual fuel element it was cropped from is unknown, since the croppings are not individually tracked in the storage basin, but a minimum operating temperature of 60°C and minimum in-reactor time at temperature of 113 days can be assumed bounding based on known MURR operating parameters [6]. Between ~6.3-day periods of operation, it would have spent periods in wet storage in a pool with a mixed bulk temperature of 37.8°C. Since its final discharge from the reactor, it has been stored in the Savannah River Site (SRS) L Basin wet storage pool (average temperature 22°C) for a period of <18 years.

The cropped portion of the assembly does not contain any fuel meat, only aluminum, but it does have a surface layer of (oxy)hydroxides formed in the reactor and/or during wet storage. A portion of the sidewall of the cropping was removed to characterize the (oxy)hydroxides, as documented in Ref. [6], and the entire

remainder of the cropping other than these characterization samples was used in the mini-canister test. The cropping was cut with bolt cutters into pieces that would fit into the canister, and Figure 2-2 (center) shows the cut pieces inside the mini-canister prior to closure. Notably, the MURR sample is much smaller than the surrogate assemblies and thus occupies a lower fraction of the mini-canister volume. The mass of the MURR pieces irradiated was 169 g. As a result of the lower sample size and correspondingly larger gas volume, the H_2 concentration measured in the canister gas was expected to rise more slowly than for the surrogate assemblies if the radiolytic yields from both samples were similar. (The MURR cropping was tested in a third mini-canister that was not used for other samples and is shown in Figure 2-2 (right).)

Figure 2-2. (Left) MURR cropping in shielded cells prior to characterization, (center) MURR cropping pieces loaded into the mini-canister, and (right) sealed MURR mini-canister with contamination filter.

2.4 Mini-canister conditioning and sealing

Once loaded with the respective sample assemblies and closed, each of the two As-Dried mini-canisters underwent a heated drying process. Each loaded vessel was placed in an oven with the mini-canister's exhaust/sample line extending out of the oven, and the sample line valve was left open to lab air to allow warm, moist air to escape the vessel. The oven was ramped up to that canister's individual target drying temperature (150°C or 220°C, depending on the canister) with the loaded mini-canister inside; once both the oven and a thermocouple on the exterior of the mini-canister reached the target temperature, it was held at that temperature for 4 hours. The characterization sample removed from the 220°C As-Dried assembly was dried in the oven alongside the corresponding canister. During drying of the 220°C As-Dried canister, liquid water was observed in the form of a bubble on the end of the sampling line (Figure 2-3). No attempts were made to collect/quantify the mass of liquid water removed. However, the observation of liquid water exiting the sample line during the 220°C treatment process does provide direct evidence of water removal from the sample. This was assumed to arise primarily from release of water chemically incorporated into the (oxy)hydroxide/corrosion layer. Following the 4 hours at elevated temperature, the oven was turned off, and the mini-canister's exhaust line was connected to a vacuum pump for 1 hour while the vessel remained in the residual heat of the oven in order to extract moist air before it cooled and the water could recondense. The vessel was then subjected to a 12-hour vacuum step at room temperature. The vacuum pump used provided a 0.02 psia (0.14 kPa) hold pressure. Prior to final backfilling with helium and sealing, the mini-canisters were subjected to a series of short, alternating helium purge/vacuum steps to eliminate any remaining residual air from the canister. The vacuum steps in the purge process lasted ~5 seconds with a target pressure of <0.1 psia (<0.7 kPa), and the gas was checked for residual N_2 and O_2 using a gas

chromatograph (GC). A total of four vacuum/purge steps were needed for the As-Dried canisters. The canisters were backfilled with dry helium to ~24 psia (166 kPa) prior to irradiation.

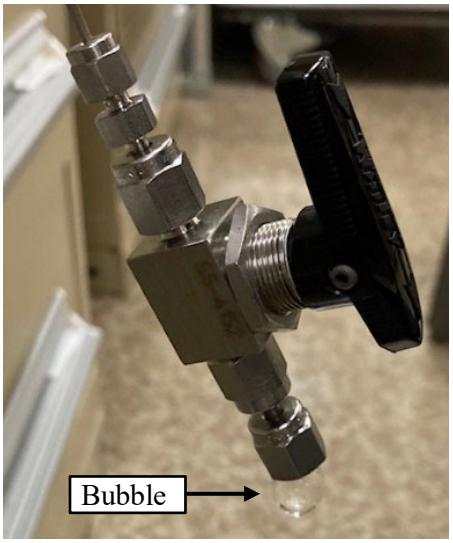

Figure 2-3. Water bubble forming at the sampling line outlet (bottom of photo, indicated by arrow) during 220°C drying process.

The As-Corroded Vacuum-Only assembly underwent the same 12-hour, room-temperature vacuum step and four helium/vacuum purges to remove residual air, without any heated drying steps. The extended vacuum step was originally intended to help remove trace amounts of air remaining in the system; however, it could plausibly remove additional adsorbed moisture as well, and later radiolysis data from ampoule experiments [3] suggested that extended, unheated vacuum did, in fact, reduce the H_2 yield compared to nominally undried samples.

As a result, the extended vacuum step was omitted from preparation of both the As-Corroded No-Vacuum and MURR mini-canisters to test them in an undried baseline state. The As-Corroded No-Vacuum assembly was air-dried for at least 16 h in a negative-pressure chemical hood which provided some airflow, while the MURR sample had been stored dry and exposed to ambient air in a rad hood since being removed from L Basin for characterization in late 2018 [6]. Elimination of residual air for these canisters was accomplished solely via the sequential helium/vacuum purge steps, with each vacuum step lasting only ~5 s rather than hours. The lack of previous drying steps was reflected in an increase in the number of required helium/vacuum purges to seven (compared to four for the dried canisters).

2.5 Mini-Canister Irradiation

The loaded and sealed mini-canisters were irradiated in the cavity of a Co-60 gamma irradiator. The original As-Corroded Vacuum-Only and 220°C As-Dried surrogate assemblies as well as the MURR sample were initially irradiated in a JLS Model 484 irradiator which had a relatively low dose rate. They were later moved to a newer FTS Model 812 irradiator with a much higher dose rate to complete the irradiation to their target cumulative dose. The 150°C As-Dried and As-Corroded No-Vacuum mini-canisters were irradiated entirely within the FTS Model 812. The data obtained in different irradiators is expected to be comparable when evaluated as a function of the accumulated dose (Gy), since previous data indicates that differences in dose *rate* (Gy/s) do not significantly alter the radiolytic yield as a function of dose. Ref. [7] reported $G(H_2)$, i.e., radiolytic H_2 yield normalized by absorbed radiation energy, for water vapor measured at four different dose rates from 1070 to 10700 Gy/s, plotted as a function of time; when replotted as a function of the dose (Gy), the different data sets fall along the same curve [8]. Similarly, comparison of

$G(H_2)$ for corroded aluminum coupons irradiated in different irradiators at different dose rates (8.3–175 Gy/min) was part of a previous "round-robin" radiolysis study, and no evidence of significant dose rate dependence was observed [9].

Fricke dosimetry was performed in both irradiator sample chambers using a large volume of solution evenly distributed throughout an otherwise empty mini-canister placed in each of the irradiation locations. Dose rates calculated in the Fricke solution were multiplied by the ratio of μ_{en}/ρ between H_2O and aluminum to account for effects of electron density on Compton Scatter probability. Resulting dose rates in the aluminum were recorded as 5.8 Gy/min in the Model 484 irradiator in February 2021 and 124 Gy/min in the Model 812 in May 2022. Reported cumulative doses that appear in the radiolytic yield plots use an integrated form of the Co-60 decay formula to account for the continuous falloff of dose rate due to predictable radioactive decay. (The impact of the decay over the course of an individual test is relatively small given the Co-60 half-life of 5.27 years.)

2.6 Gas Sampling

A gas sampling manifold was used to collect 10-mL gas samples from each irradiated vessel at intervals. For each sample, the manifold was evacuated by a vacuum pump prior to opening the valve to the mini-canister, then the valve was opened to allow the mini-canister gas to expand into the manifold volume [10, 11]. The pressure was recorded after each sample using a Paroscientific pressure transducer in the sampling manifold [10, 11]. The gas sample was automatically injected into an Inficon 3000 Micro GC Fusion Gas Analyzer equipped with a thermal conductivity detector sensor and two analytical columns. The primary GC column, used to quantify the H_2 concentration, is a 20-meter molecular sieve using argon carrier gas. The secondary column, primarily used to quantify O_2 and N_2, is a 10-meter molecular-sieve column with a helium carrier gas. Calibration gases containing various certified concentrations of H_2, O_2, and N_2 in helium were used to calibrate the GC.

Because each sample is permanently removed from the gas inventory remaining in the vessel, the calculation of total radiolytic H_2 generated included the moles of H_2 that were removed in previous samples and accounted for the changing vessel pressure as each sample was removed.

2.7 Hydrogen Concentration Spike

During the transfer of the As-Corroded Vacuum-Only mini-canister from the original JLS irradiator to the FTS irradiator (the first of the mini-canisters to be transferred), an in-line ball valve in the canister's sampling line was inadvertently placed inside the radiation field. This resulted in a rapid increase in H_2 concentration within the mini-canister. Repositioning the canister to remove the valve from the radiation field successfully ended this anomalous spike in the H_2 generation rate. This incident prematurely ended the intended As-Corroded Vacuum-Only test due to the alteration of the gas atmosphere; however, the spike of H_2 from a source external to the sample also provided an opportunity to assess the potential impact of the gaseous H_2 concentration.

Therefore, following the removal of the valve from the radiation field, the mini-canister was returned to the irradiator and monitored for an additional ~1 MGy accumulated dose to investigate whether the sudden increase in H_2 partial pressure would alter the H_2 generation rate from the sample compared to that before the H_2 spike. For example, this would provide insight into whether the general observation that the H_2 generation rate decreased over time resulted from the build-up of H_2 in the gas space suppressing further generation or was due to a different mechanism.

2.8 Post-Irradiation Heat Treatment

Post-irradiation heat treatments were applied to the two As-Dried canisters to check whether there was H_2 and/or O_2 trapped within the oxide or (oxy)hydroxide that might be released at elevated temperatures. After

each canister was irradiated to the target dose of at least 15 MGy, an oven was used to heat the still-sealed mini-canisters sequentially to 100°C, 150°C, and 200°C for one hour at each temperature. After each temperature stage, the canisters were allowed to cool to room temperature as verified by an external thermocouple, and the gas was sampled and characterized by the GC.

3.0 Results

3.1 (Oxy)hydroxide characterization

3.1.1 Surrogate assemblies

The samples removed from the As-Corroded Vacuum-Only and 220°C As-Dried surrogate assemblies were used to characterize the (oxy)hydroxide film. X-ray diffraction (XRD) was used to identify the type of (oxy)hydroxide, and planview and cross-sectional scanning electron microscopy (SEM) were used to examine the morphology and thickness of the (oxy)hydroxide film. These characterization results were reported previously [3, 2].

The XRD spectrum for the sample taken from the As-Corroded Vacuum-Only assembly (Figure 3-1, top) showed prominent, sharp peaks for bayerite as well as for the aluminum metal, along with a small, broad peak corresponding to boehmite. For the 220°C As-Dried sample (Figure 3-1, bottom), bayerite remained the most prominent (oxy)hydroxide signal, but distinct, sharp boehmite peaks also appeared, and the height of the bayerite peaks relative to the aluminum peaks was smaller for the 220°C As-Dried sample compared to the As-Corroded Vacuum-Only. The reduction in bayerite peaks and appearance of sharp boehmite peaks suggests that the 220°C, 4-hour drying process succeeded in partially converting the bayerite to well-crystallized boehmite. No corundum peaks were observed, as expected, since thermal decomposition of boehmite to alumina is associated with higher temperatures [12, 13, 14].

Cross-sectional SEM of the As-Corroded Vacuum-Only sample (Figure 3-2) showed a fairly consistent (oxy)hydroxide layer that was mostly between 5 and 10 µm thick. Thickness measurements were taken at 10-µm intervals across three different cross-section SEM images, for a total of 69 measurements; the measured thicknesses averaged 8.9 µm with a range of 4.1 to 21.2 µm.

Planview SEM of the two samples (Figure 3-3) showed near-identical (oxy)hydroxide morphologies, which appeared to consist predominantly of narrow rods of (oxy)hydroxide. Rod widths measured from different locations in an SEM image of the As-Corroded Vacuum-Only sample averaged 0.25 µm (77 measurements ranging from 0.09–0.47 µm). In some areas, these rodlike structures formed “bundles” of parallel rods which project out from the substrate at various angles, while other areas featured shorter, individual rods in seemingly random orientations. The randomly oriented patches appear to sit on top of bundles of aligned rods in at least some regions.

Comparison of the planview SEM between the two samples revealed the presence of very narrow cracks in the 220°C As-Dried (oxy)hydroxide, which were visible in several areas dominated by the aligned-rod structures with the cracks running roughly perpendicular to the aligned rods. The crack width is on the order of 0.1 µm and of similar scale to the width of isolated (oxy)hydroxide rods, making them difficult to spot. Cracking of bayerite films on aluminum with apparently unchanged morphology between cracks has been previously observed after samples were heated to and held at temperatures ≥200°C during thermogravimetric analysis [12]. This was attributed to contraction of the film as bayerite was converted into denser boehmite [12], which is consistent with previous literature information that gibbsite, another polymorph of $Al(OH)_3$, developed large internal porosity while otherwise retaining its gross morphology when thermally dried to Al_2O_3 [13, 14].

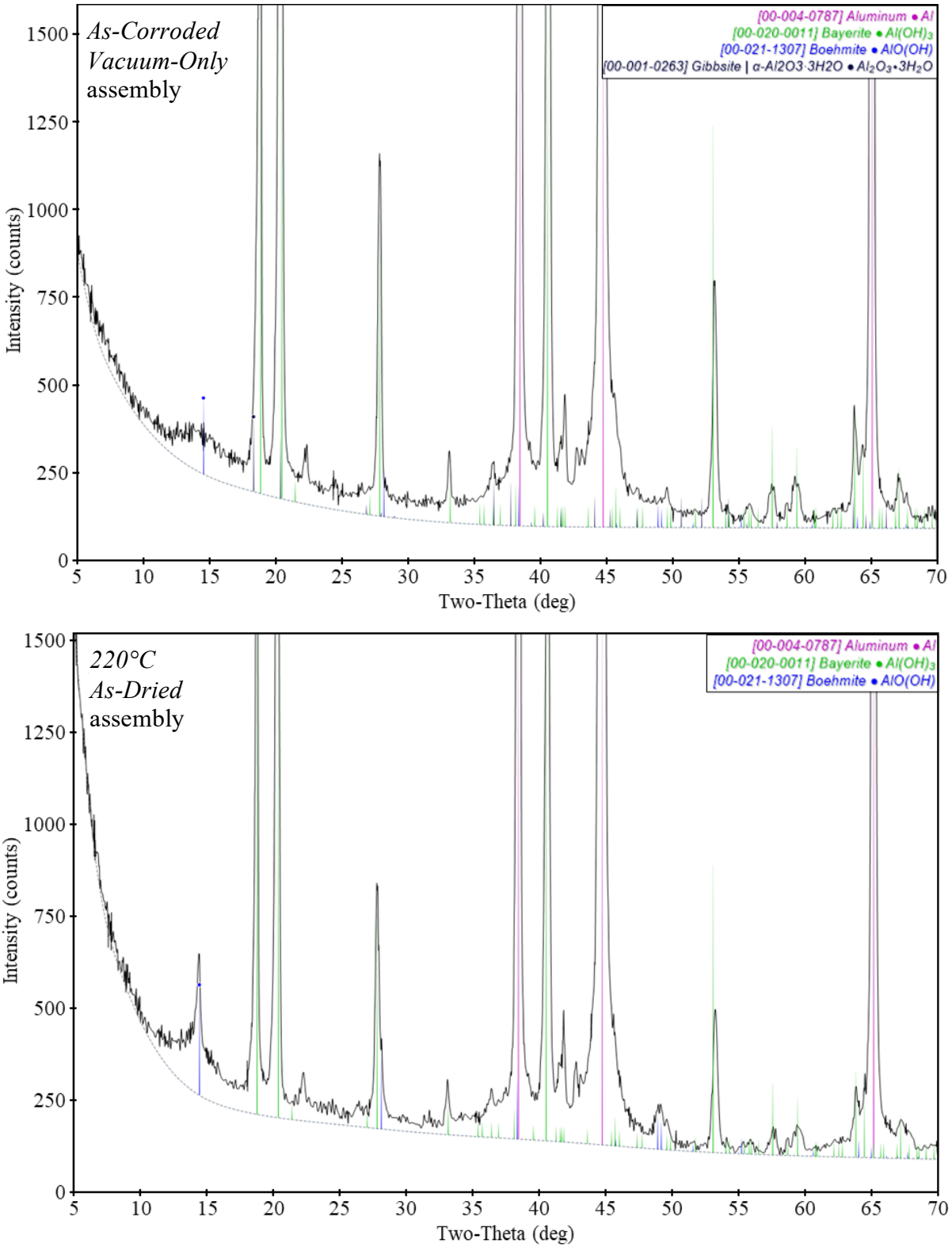

Figure 3-1. XRD spectra of the (top) As-Corroded Vacuum-Only and (bottom) 220°C As-Dried plate assembly characterization samples.

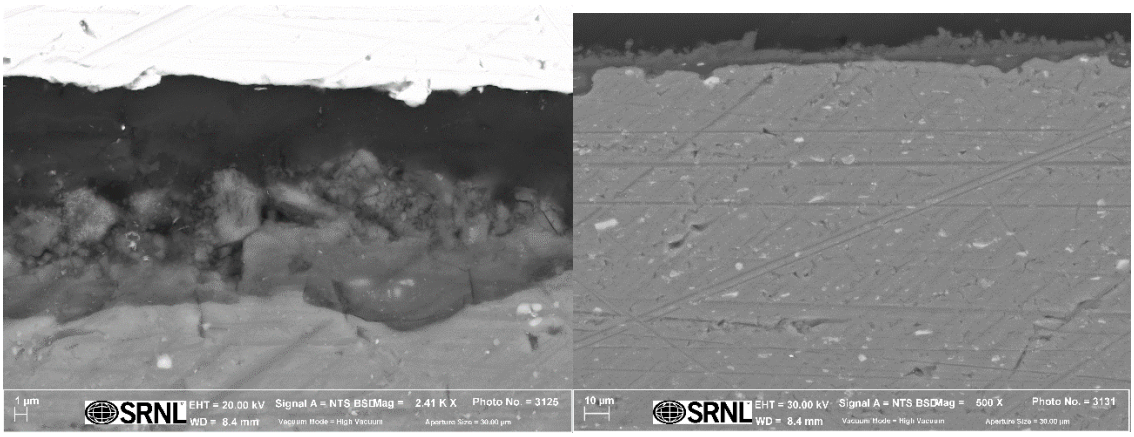

Figure 3-2. SEM cross-section images of the As-Corroded Vacuum-Only oxide layer, 5-10 µm thick.

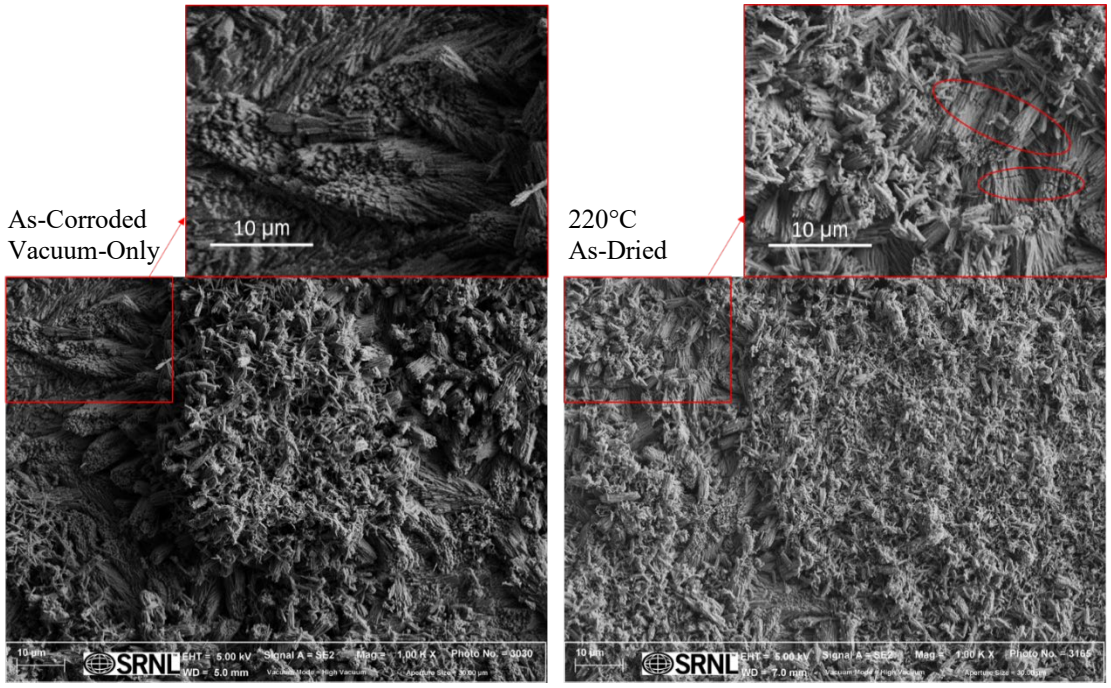

Figure 3-3. Examples of oxyhydroxide morphology from the characterization samples taken from the (left) As-Corroded Vacuum-Only and (right) 220°C As-Dried assemblies. Several fine cracks observed in the dried (oxy)hydroxide are marked with red ovals in the enlarged section at top right.

3.1.2 MURR

Samples cut from the MURR cropping were characterized as reported in [6] to determine the (oxy)hydroxide characteristics. The MURR characterization (XRD and SEM) focused on a surface that faced the inside of the fuel element in case efforts to decontaminate the outer surface prior to cutting using a soft-bristle brush had caused any disturbance of the (oxy)hydroxide condition [6].

The XRD spectrum (Figure 3-4) showed clear peaks for bayerite and aluminum metal as well as a broad boehmite peak. Planview SEM (Figure 3-5, left) showed a blocky (oxy)hydroxide characterized by flat, angular structures. Cross-sectional SEM (Figure 3-5, right) indicated that the (oxy)hydroxide layer was relatively uniform in thickness over the region examined. Thickness measurements of the imaged cross-section at 5-µm intervals (15 measurements) averaged 9.1 µm with a range of 4.2-10.7 µm (all but the 4.2-

µm measurement fell in an even narrower range of 8.3-10.7 µm). The location imaged was on the inside stepped edge of the cropping, between the grooves that would have held the fuel plates.

The observed composition (clear bayerite peaks with some indications of boehmite) and approximate thickness (averaging ~9 µm) were similar between the surrogate assemblies and the MURR cropping, despite their differences in morphology as seen in planview.

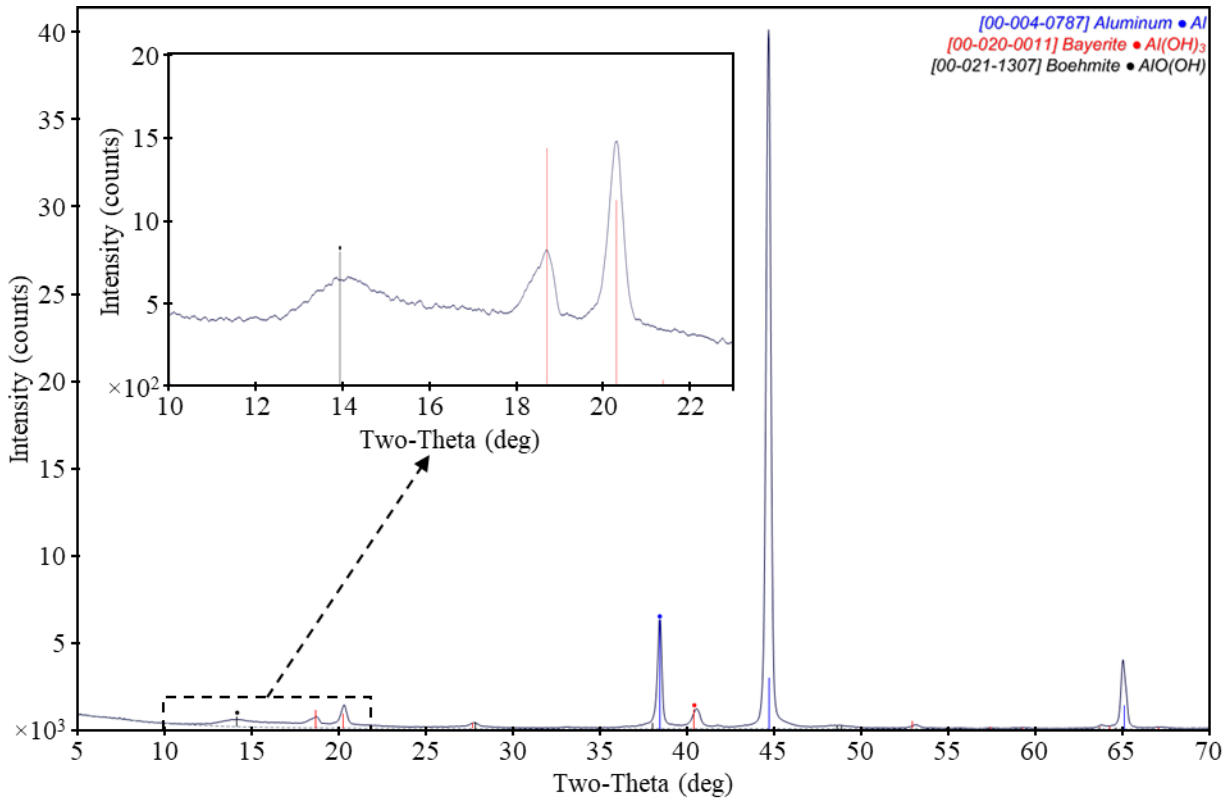

Figure 3-4. XRD spectrum for the MURR sample.

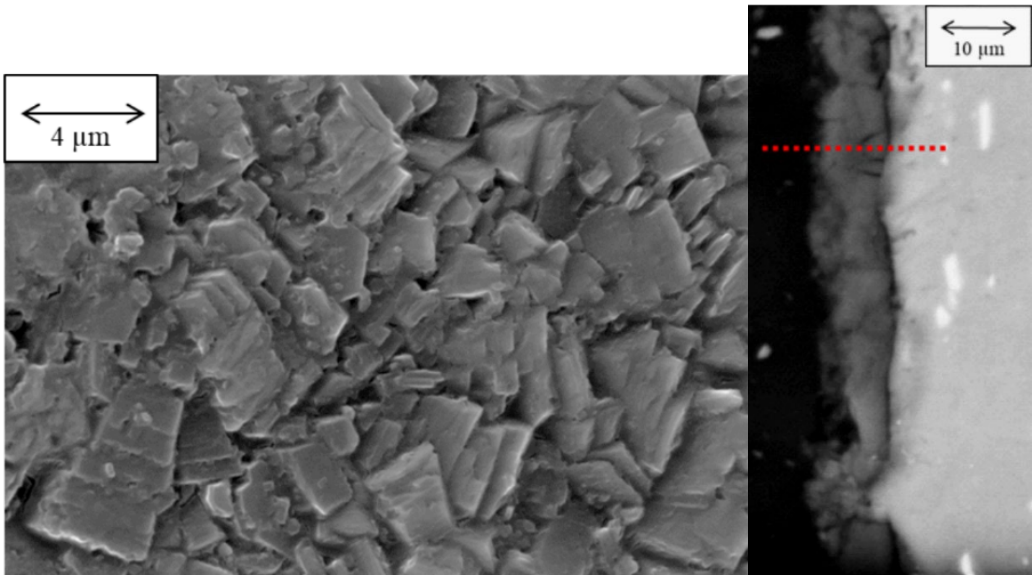

Figure 3-5. Planview (left) and cross-sectional (right) SEM of MURR sample.

3.2 Mini-canister radiolysis results

Figure 3-6 shows the cumulative H_2 generation in µmol as a function of absorbed dose for the four surrogate assemblies and MURR. The top plot includes the entire range of the data, while the bottom plot narrows the vertical axis to focus on the lower-yield results. All mini-canisters except the As-Corroded Vacuum-Only were irradiated to a dose of at least 15 MGy; the As-Corroded Vacuum-Only assembly reached only ~1.5 MGy before the inadvertent H_2 spike, and only the pre-spike data is plotted in Figure 3-6. (The data is also provided in tables in Appendix A.)

The two As-Corroded mini-canisters appear to show very similar H_2 generation rates in the low-dose region where they overlap, suggesting negligible impact from the extended vacuum step on the initial H_2 yields. The slope of the As-Corroded Vacuum-Only data set was ~320 µmol/MGy in the very low-dose range (up to ~0.1 MGy) and quickly decreased to ~120 µmol/MGy in the 0.4–1.5 MGy range[1], while the early slope of the As-Corroded No-Vacuum data (0.5-3.5 MGy range) was ~155 µmol/MGy. Unfortunately, due to the early end of the As-Corroded Vacuum-Only test, it is unknown whether the extended vacuum would provide a reduction in yield at higher doses in the 2–15 MGy range, but at its final dose, it was ~85% of the yield for the As-Corroded No-Vacuum canister. The As-Corroded No-Vacuum yield appears to transition to a lower slope around roughly 6–7 MGy, but the H_2 yield continued to grow roughly linearly up to the maximum dose tested at ~15 MGy with a slope of ~66 µmol/MGy.

Corroded No-Vacuum assembly, and this reduction was evident from the beginning of the irradiation test. The 150°C and 220°C As-Dried assemblies also show similar rates of H_2 generation to one another over the dose range tested, despite the 220°C As-Dried being expected to harbor less chemisorbed moisture due to its drying temperature reaching the bayerite-to-boehmite transition temperature. Figure 3-6(bottom) shows sample H_2 yields over a narrower range of yield to more clearly show the behavior of the lower-yield As-Dried and MURR mini-canisters. The final yields for the 150°C As-Dried were actually lower than those of the 220°C As-Dried, despite the lower drying temperature. However, the mass gain of the 150°C As-Dried assembly during corrosion was also lower (Table 2-1), only 81% of that for the 220°C As-Dried assembly; the difference in mass gain is of similar magnitude to the difference in H_2 yield at the 15 MGy dose.

The two As-Dried mini-canisters displayed their highest H_2 generation rates at the beginning of the irradiation (fitted slopes for 0–6 MGy of ~34 µmol/MGy for 150°C As-Dried and ~38 µmol/MGy for 220°C As-Dried) and transitioned to a lower slope at higher doses (~6 µmol/MGy for both As-Dried samples). Neither displays an unambiguous plateau before reaching 15 MGy. Similar to the As-Corroded No-Vacuum, the most prominent change in slope appears to start above roughly 6 MGy. Both the initial and final H_2 generation rates were significantly lower than those for the As-Corroded canisters.

The H_2 yield of the MURR mini-canister is the lowest of all of the samples for most of the dose range tested, despite being in a nominally undried state, but it is also much smaller than the surrogate assemblies (only 169 g compared to 617–640 g surrogate assemblies). As for the surrogate assemblies, the MURR's highest H_2 generation rate occurred at the beginning of irradiation with a fitted slope of ~38 µmol/MGy up to 0.6 MGy. The H_2 generation rate decreased to a lower rate by ~2 MGy, and the yield between ~2 and 13 MGy appears to be roughly linear with slope ~18 µmol/MGy; finally, there appears to be a further slight reduction in generation rate in the ~13–15 MGy range with slope ~6 µmol/MGy (Figure 3-6, bottom).

[1] The slopes for the lowest dose ranges were fitted with zero intercept, while the higher dose ranges were fitted with non-zero intercepts.

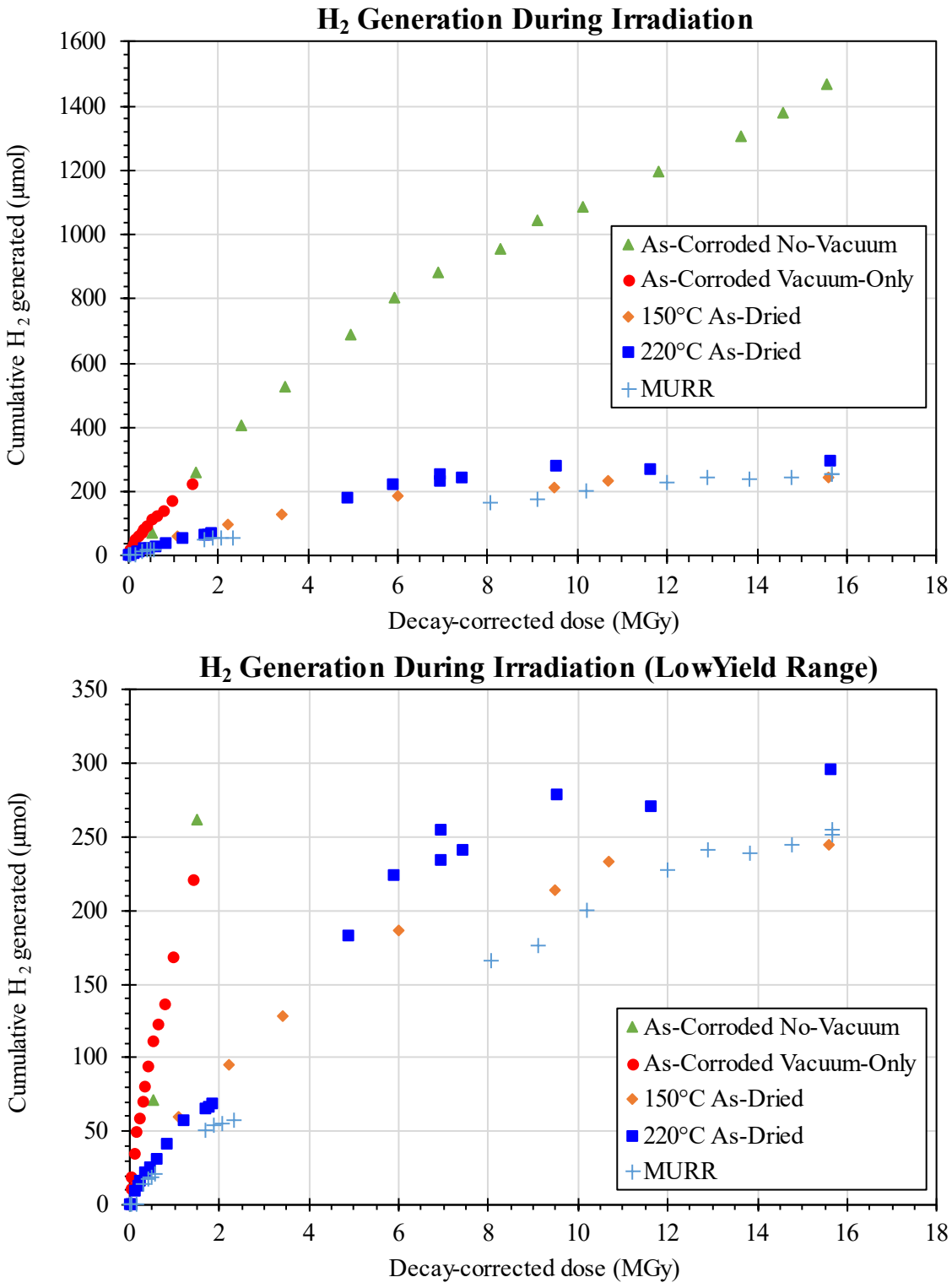

Figure 3-6. Cumulative radiolytic H2 yields from mini-canister experiments (top) for the full data range and (bottom) zoomed in on the vertical axis to more clearly show the lower-yield data.

Both the 150°C and 220°C As-Dried assemblies show significantly lower H_2 generation rates compared to the two As-Corroded assemblies without heated drying, with yields around 20% of the yield from the As-

Figure 3-7 normalizes the H_2 yields (top) by the total mass of the sample and (bottom) by the (pre-drying) mass of the oxide estimated from the corrosion mass gain (Table 2-1) assuming it corresponded to formation of bayerite. The MURR cropping data is omitted from the oxide-normalized plot (Figure 3-7, bottom) because the corrosion mass gain is not available for the service-formed oxides.

There was little variation in total mass among the four surrogate assemblies (617–640 g), so the normalization by sample mass (Figure 3-7, top) makes little difference in their relative yields, but it makes a large difference in the relative yield for the small (169 g) MURR sample. When normalized by the sample mass, the MURR yield is about two-thirds of that for the As-Corroded No-Vacuum, which is its closest analogue in preparation, i.e., nominally undried. They also featured similar slopes when normalized by sample mass: Initial low-dose slopes of ~0.24 μmol/(g·MGy) for As-Corroded No-Vacuum up to 3.5 MGy and ~0.23 μmol/(g·MGy) for MURR up to ~0.5 MGy and higher-doses slopes of 0.10 μmol/(g·MGy) for both the As-Corroded No-Vacuum at > 6 MGy and the MURR for ~2–10 MGy.

The relative differences in estimated bayerite mass among the surrogate assemblies was larger, so the normalization by oxide mass (Figure 3-7, bottom) does have a notable effect on their relative yields. Corrosion mass gains ranged from 5.5 g for As-Corroded Vacuum-Only to 4.3 g for the 150°C As-Dried and As-Corroded No-Vacuum (Table 2-1), corresponding to up to 28% difference in estimated bayerite mass. When normalized by bayerite mass, the difference in yield between the 150°C and 220°C As-Dried assemblies essentially disappears. By contrast, the As-Corroded Vacuum-Only yield at its maximum dose (~1.5 MGy) diverges further from the As-Corroded No-Vacuum at the same dose point, corresponding to about two-thirds of the As-Corroded No-Vacuum yield per unit oxide mass.

Although both N_2 and O_2 are monitored for in each gas sample, no generation of gaseous O_2 was detected during any of the mini-canister irradiations. This is consistent with other experimental investigations by SRNL, Idaho National Laboratory (INL), and others [15]. The lowest concentration of O_2 for which calibration was performed is 510 ppm. Calculated O_2 concentrations never exceeded this value during the radiolysis or post-irradiation heat treatment tests (for comparison, H_2 yields exceeded 7000 ppm for all mini-canisters). No trend of increasing O_2 with increasing dose that would suggest radiolytic generation was observed during irradiation. Some GC samples did include detectable levels of O_2 below the calibration threshold, but these measurements fluctuated independently of dose, and the observations are consistent with residual O_2 in the sampling manifold following extended periods of inactivity between purges. Same-day sequential sampling consistently resulted in low O_2 signal of similar magnitude for all doses and heat treatment conditions; these low amounts of O_2 are estimated to be ~100 ppm based on extrapolation of the calibration curve, but the exact amount cannot be confirmed without additional calibrations using certified gas mixtures with lower than 510 ppm O_2.

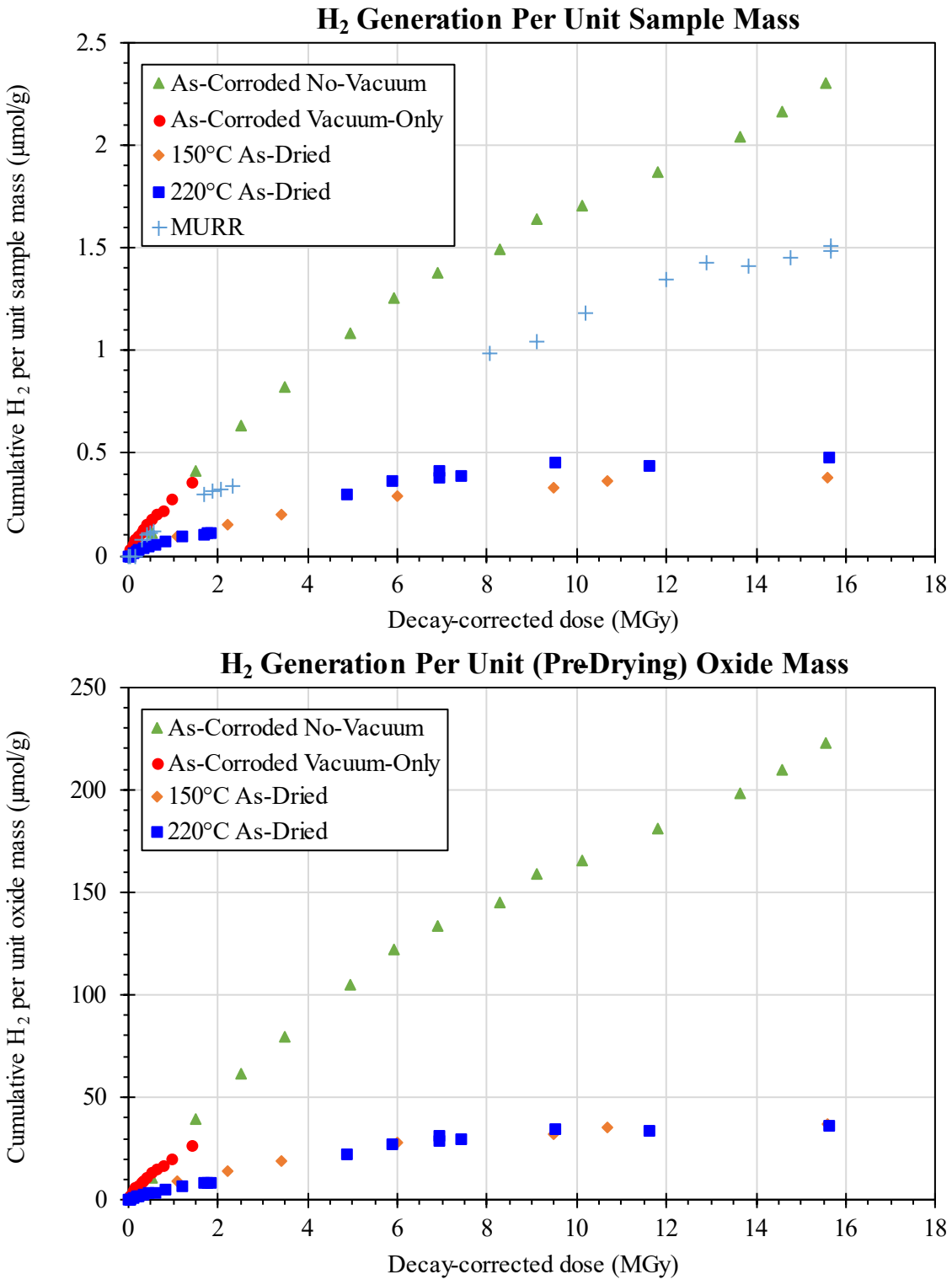

Figure 3-7. Cumulative radiolytic H_2 yields normalized by (top) the total sample mass and (bottom) the estimated (pre-drying) oxide mass based on corrosion mass gain.

3.3 Hydrogen spike in As-Corroded Vacuum-Only mini-canister

The spike in H_2 due to irradiation of the valve resulted in the H_2 gas fraction increasing rapidly from 0.8 vol% (prior to the move to the new irradiator) to 13 vol% over <2 MGy increase in dose. To compare the yields from the sample before and after the increase in H_2 concentration in the gas, Figure 3-8 plots the cumulative H_2 yield measured after removing the valve from the radiation field, i.e., starting from the 13% H_2 reading as the zero point for the "Post-spike" generation, along with the original As-Corroded Vacuum-Only data ("Pre-spike"). The overall H_2 generation rate following the sixteenfold increase in H_2 concentration is very similar to that pre-spike, indicating no significant suppression by the addition of H_2 gas to the canister. Therefore, observed decreases in H_2 generation rate with increasing dose and any potential "roll-over"/plateauing effect do not seem to be caused by the elevated gaseous H_2 concentration and instead must be driven by another mechanism.

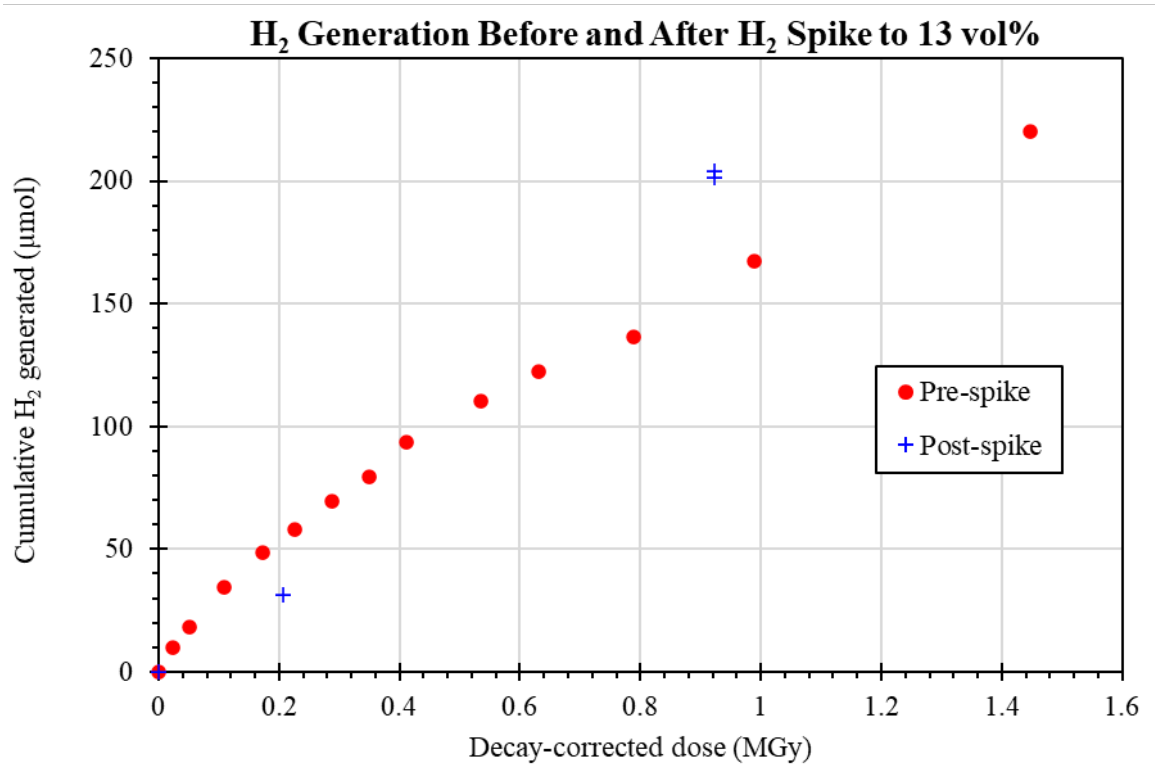

Figure 3-8. Radiolytic H_2 yields from the As-Corroded Vacuum-Only mini-canister before and after the H_2 concentration increased 13 vol%.

3.4 Post-irradiation heat treatments

Post-irradiation heat treatments of both As-Dried mini-canisters were performed after they reached over 15 MGy absorbed dose. A study by Kaddissy et al. [16] of aluminum (oxy)hydroxide powders exposed to electron beam irradiation found that some of powders released additional radiolytic H_2 after post-irradiation heating to elevated temperatures (up to 250°C). If such a trapping mechanism occurred in the mini-canister assemblies, it was speculated that the amount of trapped H_2 might differ between the 150°C and 220°C As-Dried samples due to their different drying conditions. Exposing the canisters to furnace air temperatures of 100°C, 150°C, and 200°C for an hour at each temperature post-irradiation did not show a significant effect on the cumulative H_2 yield measured from either canister. No more than a 5% difference in calculated H_2 yield and no consistent trend of increasing or decreasing H_2 was observed across the post-irradiation heat treatments of an individual mini-canister (Table 3-1). The Room Temp. H_2 values correspond to the end of initial irradiation testing from Table 7-4 and Table 7-3. These variations could have been due to

instrument uncertainty or variations in the internal container temperatures across different samples, although the external canister surface was allowed to cool to room temperature (22°C–24°C) prior to each gas sample.

Table 3-1. Post-irradiation heat treatment H_2 yields from As-Dried mini-canisters.

Post-Irradiation Heat Treatment	Total μmols H_2 produced over test	
	150°C As-Dried	220°C As-Dried
Room Temp.	245	296
100°C for 1 hr	249	311
150°C for 1 hr	246	306
200°C for 1 hr	252	307

O_2 gas was measured for each post-irradiation gas sample, as during the primary irradiation period. No evidence of O_2 release during the heat treatments was observed.

4.0 Discussion and Model Implications

In addition to the mini-canister data, radiolysis measurements have also been conducted on irradiated samples in flame-sealed glass ampoules, which were initially chosen to minimize impacts from interaction between the gamma radiation and/or radiolysis products with the vessel material [3]. Ampoule-based testing has been conducted by both SRNL and INL, some of which have also investigated the impacts of drying steps [3, 17] and will be used for comparison here. In contrast to the mini-canister tests, ampoules provide only one data point per sample since the ampoule must be cracked open to collect the gas after accumulating the prescribed dose. Compiling the yield curves from many small samples lends itself well to collection of duplicate measurements to capture the impact of minor variations in the sample conditions and/or preparation, but this also tends to result in relatively high scatter in the yield curves compiled from individual samples compared to the mini-canister data that follows a single sample and preparation condition over the full dose range.

4.1 Physical interpretation

4.1.1 Free, physisorbed, and chemisorbed water and the impact of drying processes

Three potential reservoirs of residual water are expected to be relevant for these experiments and for ASNF sealed dry storage: residual free water (e.g., traces of water vapor or, in a full-scale canister, trapped liquid water or ice in occluded areas), physisorbed water adsorbed to various material surfaces, and the chemisorbed/chemically bound water corresponding to the aluminum (oxy)hydroxides.

When the radiolysis test campaign was initiated, the aluminum (oxy)hydroxides were expected to be the primary water source impacting the H_2 yield, particularly after the application of an active vacuum or heated drying step. However, the results of radiolysis testing suggest that physisorbed water plays a more prominent role than expected in early radiolytic H_2 yield. For example, ampoule tests have shown lower H_2 yields for ampoules exposed to longer unheated vacuum steps during preparation [3]. These ampoules were loaded dry with drip-dried/air-dried samples, so no significant liquid water should have been present, and unheated vacuum is not expected to decompose aluminum (oxy)hydroxides; therefore, only the phyisorbed water is expected to be removed by such a drying step. Similarly, the 150°C and 220°C As-Dried assemblies exposed to heated drying conditions displayed a large reduction in H_2 generation rate/yield compared to those without heated drying, but the 220°C As-Dried assembly did not display a further reduction in yield (relative to the 150°C As-Dried) up to 15 MGy despite reaching the bayerite decomposition threshold of

220°C. Since significant removal of chemisorbed water is expected only for the 220°C drying condition, this suggests that the primary impact of heating on the yields within this dose range was the removal of more physisorbed water. The importance of physisorbed water is also supported by the results of ampoule tests showing that 1) the yields of undried "pristine" samples not corroded to produce an (oxy)hydroxide were comparable to or exceeded those with boehmite or bayerite films in the low-dose range and 2) lower H_2 yields were observed after heated drying of "pristine" samples at 200–350°C or of samples with boehmite films (not expected to thermally dehydrate below ~400°C [12, 13]) at temperatures of 150-200°C [3].

The (oxy)hydroxide characterization (Figure 3-3) showed that the lab-grown bayerite films comprised very small structures, giving them a high microscopic surface area to hold physisorbed water relative to the nominal surface area of the samples. However, even considering the high microscopic surface area, the amount of physisorbed water on the (oxy)hydroxide surface is still estimated to be much lower than the total chemisorbed water contained in the (oxy)hydroxide films.

4.1.1.1 Estimation of physisorbed and chemisorbed water content on surrogate assemblies

Assuming each monolayer of water corresponds to 0.3 mg/m^2 (upper end of the range reported by Ref. [18]), each monolayer on the nominal surface area of the surrogate assemblies (~3800 cm^2) would correspond to just 0.114 mg or 6.33 µmol water. The actual surface morphology of the bayerite appears to consist of rodlike structures ~0.25 µm in diameter, and the corrosion mass gains of 4.3–5.5 g correspond to an estimated 6.6–8.4 g of bayerite (density 2.53 g/cm^3). In the bounding case that all of the bayerite mass took the form of isolated 0.25-µm-diameter cylinders, the circumferential surface area (neglecting the ends) would be ~42–53 m^2, about 110–140 times the nominal surface area of the samples. Each monolayer of water on 42–53 m^2 corresponds to ~12–16 mg or ~700–900 µmol water. Since the (oxy)hydroxide rods touch and form a connected film rather than isolated particles, the actual surface area is expected to lie between these two extremes, i.e., corresponding to between ~6 µmol water and ~700–900 µmol water per monolayer. By comparison, 6.6–8.4 g of bayerite (4.3–5.5 g corrosion mass gain) would contain 2.3–2.9 g or 0.13–0.16 mol (130,000–160,000 µmol) chemically bound H_2O, exceeding the estimated physisorbed water in one monolayer on even the estimated bounding surface area by two orders of magnitude.

4.1.2 Vacuum vs. heated drying

The results of the mini-canister experiments (Figure 3-6 and Figure 3-7) indicate that the impact of 12-h unheated vacuum drying on the initial H_2 generation rate was small (at least in the relatively low-dose region where there is data), while the two heated drying conditions reduced the H_2 generation dramatically from the beginning of the irradiation. (Note that the heated drying conditions also included an extended vacuum after the heated step.) It is interesting to compare these to data from other tests to see whether the pattern of a greater reduction in H_2 generation holds more generally.

Ref. [3] reported the results of testing various surrogate coupons in glass ampoules under dry argon cover gas, including testing the impacts of both unheated vacuum drying and heated drying steps. These experiments include direct comparison of yields after various vacuum or heated drying conditions against corresponding air-dried/nominally undried coupons but did not include direct head-to-head testing of vacuum vs. heated drying for equivalent coupons and doses. Table 4-1 summarizes the relative H_2 yields of dried samples as a percentage of the yield measured for directly comparable undried samples, i.e., same kind of test/sample (ampoule vs. mini-canister), same (oxy)hydroxide type, and approximately the same dose, for both the ampoule data and the mini-canister tests.

For "pristine" coupons expected to have only a very thin Al_2O_3 film and no (oxy)hydroxides, heated drying for 4 hours at 200°C or 350°C reduced their H_2 yields (at 67 kGy) to 61% and 30% of the undried yield, respectively [3, 19]. Even the 350°C drying did not reduce the yield to zero, as would be expected if all physisorbed water were removed from a coupon without (oxy)hydroxide; these samples were exposed to

ambient air for ~5–10 minutes between drying and backfilling with dry argon, so it is unknown whether adsorbed water survived the drying process or was readsorbed [3, 19]. A 12-h vacuum-drying step for similar pristine coupons reduced the H_2 yield (in an estimated 0.2–0.4 MGy range) by a smaller margin, to about 71–80% of the undried yield depending on the dose point compared [3, 19].

For coupons with a well-crystallized boehmite film, heated drying for 4 hours at 150°C and 200°C (both well below the temperatures expected to dehydrate boehmite) reduced the H_2 yield to 78% (for 150°C at 1.9 MGy) and 44% (for 200°C at 1.1–1.2 MGy) of the undried yield, respectively [3, 19]. Initially, this suggests a greater drying effectiveness from the higher temperature; however, some of the coupons dried at 150°C also had the highest corrosion mass gains among the coupon set, i.e., the largest amount of oxide and potentially larger surface area due to the oxide structures. When normalized to account for this difference, the yield per unit oxide mass corresponded to 39% of the undried yield for coupons dried at 150°C and less than 46% of undried yield for those dried at 200°C, i.e., very little difference between the two drying temperatures [3, 19]. Unfortunately, there was no direct comparison of yields for boehmite-filmed coupons after vacuum drying relative to undried coupons; however, a 72-h vacuum step reduced the yield (at an estimated 0.2 MGy) to just 19% of the yield after a mere 4-h vacuum step [3, 19]. The reported dose in these vacuum tests was estimated to have potentially up to 20% error due to the proximity of the ampoules to the Co-60 sources being closer than the dosimeter measurements. Therefore, the range of yields from undried coupons from another data set for doses from 184–284 kGy [3], corresponding to roughly ±20% of the estimated dose (235 kGy) of the vacuum-dried coupons, was used as a benchmark to estimate the reduction in yield after vacuum drying. The relative yields suggest that the 4-h and 72-h vacuum steps reduced the yield to <45% and <8% of the undried yield, respectively.

Finally, pieces of the characterization samples from the As-Corroded Vacuum-Only and 220°C As-Dried assemblies were also tested in glass ampoules [3]. The 220°C As-Dried sample was dried in the oven alongside the canister but lacked the subsequent 12-h vacuum and was handled in ambient air between drying and irradiation. The As-Corroded Vacuum-Only sample was cut from the assembly prior to vacuum drying and thus corresponded to an undried state. The average yield from the 220°C-dried characterization samples (at 1.2 MGy) was only 42% of the average yield for the undried samples at roughly the same dose, i.e., a substantial reduction in H_2 yield was observed despite the handling of the dried sample in ambient air with possible readsorption of water [3, 19]. (The yield of the 220°C As-Dried mini-canister, which was not reexposed to ambient air after drying, was only ~20% of the corresponding air-dried mini-canister.) Subjecting pieces of the As-Corroded Vacuum-Only sample to 12-h vacuum (the same as the corresponding mini-canister), reduced the average H_2 yield (at estimated 0.2–0.4 MGy) to 40-56% that of the undried samples depending on the dose point considered [3, 19]. Notably, this is a larger relative reduction in yield than was observed for the As-Corroded Vacuum-Only mini-canister, which represented the same applied drying conditions.

Table 4-1. Summary of H_2 yields for dried samples relative to comparable undried samples observed in SRNL ampoule tests (argon cover gas) [3] and mini-canister tests (helium cover gas).

	Test type	Ampoules [3]						Mini-canister
	(Oxy)hydroxide	None		Boehmite		Bayerite		Bayerite
Heated drying	Drying temp. (°C)	200	350	150	200	220*		150–220
	H_2 yield relative to undried	61%	30%	78% (39% based on oxide**)	45% (46% based on oxide**)	42%		~20%
	Dose range (MGy)	0.07		1.9	1.1-1.2	1.2		0–16
Vacuum drying	Duration	12 h		4 h	72 h	12 h		12 h
	H_2 yield relative to undried	80%	71%	31-45%***	6-8%***	56%	40%	≥85%
	Dose range (MGy)	0.2	0.4	0.2***	0.2***	0.2	0.4	~1.5

* Sample handled in ambient air post-drying.
** Based on comparing normalized yield in mol per g oxide instead of total moles generated.
*** Dried yield compared to undried yields in the 235 kGy ± 20% range due to uncertain dose for the vacuum-dried coupons.

Ref. [17] similarly reported on INL radiolysis testing of surrogate samples with bayerite films in glass ampoules following application of drying steps. In contrast to Ref. [3], this study directly compared yields for unheated and heated drying steps but did not include a direct air-dried/nominally undried comparison for the same sample type. Three drying conditions were tested, all performed under rough vacuum ("≤ 22.5 in. Hg") in the same vacuum oven: 1) unheated vacuum drying overnight, 2) 100°C drying with the oven held at 100°C for 4 h and samples left to cool overnight under vacuum, 3) 220°C drying with the same procedure as 100°C drying except for oven setpoint [17]. After drying, the samples were flame-sealed into glass ampoules backfilled with dry helium. These experiments showed negligible differences in yield between the three drying conditions at doses up to ~53 MGy [17]. The average yield for the 100°C drying condition was the smallest at all three dose points where all three were tested, and its reported fitted "steady state" yield was the smallest, but the error bars on the data were larger than the differences in average yield between the different conditions. The yields per unit sample mass for all three ampoule drying conditions were 1) similar to those of an air-dried (INL) coupon corroded under different conditions and 2) larger than those measured for the 150°C and 220°C As-Dried mini-canisters [17].

The reason for the variation in observed impact of vacuum and heated drying steps on the H_2 yield is currently undetermined. Of the available data, the mini-canisters appeared to show both lower relative reduction in H_2 yield from unheated vacuum (~15% reduction at the highest As-Corroded Vacuum-Only dose) and higher impact of heated drying (~80% reduction) relative to the corresponding air-dried condition compared to SRNL ampoule data.

As previously mentioned, evidence points to much of the early/initial radiolytic yield being attributable to the physisorbed water, while the (oxy)hydroxide is believed to be a much larger reservoir of water/hydrogen. Aside from potential impacts on the radiolytic H_2 generation rate, heated drying at a temperature that can dehydrate aluminum trihydroxides such as bayerite remains the only obvious approach to reduce the inventory of chemically bound water in the canister to ensure it cannot release H_2 (or be released as molecular water in the case of thermal excursions) during long-term storage.

4.1.3 Potential plateauing of H_2 generation

Given a long-enough observation time, net radiolytic H_2 generation from a material in a sealed system (whether a laboratory sample or an actual ASNF-in-canister system) must cease, leading to a plateau in the curve of generated H_2. Physically, this is inevitable due to the finite quantity of hydrogen inside the sealed system—if no other mechanism stops the radiolysis process, then eventually all hydrogen-containing material will break down under irradiation and net radiolytic generation of H_2 will cease due to a lack of source material. This extreme possibility is captured by bounding evaluations that assume all hydrogen in the sealed canister enters the gas phase as H_2 [20].

In laboratory radiolysis testing, a fairly consistent observation is that the maximum H_2 generation rate occurs at the beginning of the irradiation and the generation rate tends to decrease with increasing dose; in some cases, with a large enough decrease that it appeared to already be entering a plateau in H_2 yield. There are multiple physical mechanisms that theoretically could slow and eventually limit the net H_2 generation. These include possibilities such as back-reactions that reach an equilibrium with the radiolytic breakdown, depletion of specific water reservoirs (e.g., physisorbed), changes in the (oxy)hydroxides or other materials that make radiolytic H_2 release less favorable, and/or a decrease in the radiation dose rate over time. (The latter is expected to occur in real ASNF dry storage canisters over the long-term, i.e., decades of interim storage and/or eventual permanent disposition in a repository, as the fuel decays.)

The observed decrease in H_2 generation rates as the absorbed cumulative gamma dose increased coincided with increasing H_2 concentration in the gas phase. As a result, one hypothesis was that elevated H_2 in the gas phase tended to drive back-reactions so that the system approaches an equilibrium as the H_2 builds up. However, experimental data suggests this is not the case.

A comparison of 1/16”-thick AA1100 coupons versus 0.01”-thick foils in the same glass-ampoule configuration under argon [3] observed no significant increase in H_2 yield from (single) boehmite-bearing coupons in the 0.7–1.8 MGy dose range with total H_2 yield of ~0.1–0.2 µmol, but ampoules containing 8 AA1100 foils apiece continued to generate H_2 over this dose range, reaching up to 0.6 µmol. Therefore, the (unknown) plateau concentration for the ampoules containing foils is clearly significantly larger than that for the coupons (although the equilibrium concentration could potentially be higher due to an increase in the forward radiolysis reaction due to the higher surface area).

The H_2 spike in the As-Corroded Vacuum-Only mini-canister provides more direct evidence that increasing H_2 in the gas phase does not reduce the net H_2 generation rate. The inadvertent irradiation of the valve resulted in a sixteenfold increase in the H_2 concentration (from 0.8 to 13 vol%) with no apparent decrease in H_2 generation rate when comparing the pre- and post-spike data (Figure 3-8).

4.2 Implications for storage and canister models

4.2.1 Impacts of drying and amounts of residual water

In an actual dry storage canister, industrial drying processes are expected to reduce the amount of free water to very low quantities by ensuring evaporation of liquid water and by applying drying criteria that limit water vapor at the end of drying to below a prescribed threshold (typically 3 Torr partial pressure) [19, 21]. However, the drying criteria are designed around free water. They relate directly to the water vapor content and are intended to also rule out liquid water since the thresholds are well below the saturation pressure at room temperature, so liquid water in contact with the gas phase should evaporate. As a result, the existing drying criteria for (commercial) SNF dry storage are not expected to impose any limitation on the amount of chemisorbed water (e.g., (oxy)hydroxide), and the amount of physisorbed water that may remain post-drying is not established and likely dependent on the specific materials with physisorbed water layers and their surface areas (including the surface area of microscopic structures and roughness).

Radiolytic yields measured at SRNL for undried vs. dried samples in both mini-canisters (Figure 3-6) and glass ampoules [3] have indicated that drying steps (either extended vacuum drying or heated drying) can result in a significant reduction in H_2 generation rates and/or yields. These experiments were all loaded in an air-dried state (no liquid water), experienced vacuum/inert gas purges which would remove residual air and existing water vapor, and were backfilled with dry inert gas. Reductions in yield were observed for both unheated vacuum (for glass-ampoule tests [3]) and for heated drying at temperatures not expected to decompose the (oxy)hydroxides (for 150°C As-Dried mini-canister test and for glass-ampoule tests [3]). This suggests that the observed impacts were related largely to removal of physisorbed water.

The evidence of drying impacts on the H_2 generation rates is mixed. The ampoule tests from [3] found that either extended unheated vacuum or heated drying significantly lowered H_2 yields relative to undried samples. By contrast, the mini-canister data (Figure 3-6) observed minimal-to-no reduction in the overall H_2 yield or yield per unit sample mass for 12-h unheated vacuum relative to the nominally undried sample over the low-dose range where data existed for both, but observed a large reduction of yield from both 150°C and 220°C heated drying. Glass-ampoule-based testing by INL [17] of samples with bayerite films dried in a vacuum oven at rough vacuum ("≤22.5 in. Hg"), either unheated or set to 100°C or 220°C, observed minimal difference between H_2 yields from the different preparation methods and the yield per unit sample mass also overlapped with that for an air-dried sample corroded under different conditions, which they interpreted to mean that none of the drying approaches reduced the H_2 generation rate [17].

Ref. [20] performed a bounding pressure analysis for a DOE Standard Canister configuration believed to represent the highest ratio of fuel surface area to free gas volume of all proposed loading configurations (not including any fillers such as neutron absorbers) to determine whether the amount of residual water would threaten the canister integrity if fully broken down by radiolysis. They concluded that release of H_2 from all chemisorbed water in a 25-µm average bayerite film on the fuel in that configuration would remain within the permissible pressure range for the DOE Standard Canister if the temperature remained below 316°C, assuming only the H_2 entered the gas phase as observed experimentally [20]. (An initial boehmite film of the same 25-µm thickness contains less water/hydrogen than the bayerite and thus provides less potential pressure build-up.) Dehydrating a 25-µm bayerite film to boehmite prior to backfilling and sealing could remove up to two thirds of the initial chemisorbed water, and heated drying to at least 220°C remains the only known method to accomplish this.

4.2.2 Modeling of radiolytic yield

The observed radiolysis behavior for samples resembling ASNF is unfortunately complex and defies a simple, clear-cut model such as a straightforward G-value. However, the data acquired to date does provide a variety of observations to be considered in modeling efforts, including the following:

- The radiolytic H_2 generation rate decreases with increasing dose. This phenomenon was observed consistently for all mini-canister tests (surrogate assemblies with all four preparation conditions and MURR cropping) and also observed for testing in glass ampoules where a data set is built up from the yields observed in many different samples irradiated to different doses, e.g., [17, 22].

- Increased concentration of gaseous H_2 does not significantly inhibit radiolytic H_2 generation (Figure 3-8 and [3]).

- Radiolytic H_2 yields, at least in the low-dose range, are dependent on the type of cover gas. E.g., yields under N_2 or helium were lower than those under argon, with the lower yield attributed to interactions with the gas (chemical reactions and Penning ionization, respectively) [23, 24].

- Multiple pieces of evidence point to physisorbed water rather than chemisorbed/(oxy)hydroxide playing a major role in the initial/low-dose radiolytic H_2 yield.

- Initial (low-dose) H_2 generation from samples without (oxy)hydroxide films can be comparable to that of samples with (oxy)hydroxide films multiple microns thick [3, 25].
- The radiolytic H_2 yield depends on the humidity in the cover gas, with moderate-to-high humidity giving higher yields than very low (0-1% RH) humidity for samples both with and without an (oxy)hydroxide film [25].
- In tests showing substantial reduction in H_2 yield from drying processes (Figure 3-6, [3]), drying processes that are not expected to thermally dehydrate the (oxy)hydroxide remain effective in reducing the H_2 generation rate, and drying processes that do partially dehydrate the (oxy)hydroxide did not show additional reduction (Figure 3-6 and Figure 3-7).

- Very limited early data suggests that high temperature (200°C) *during* irradiation (not pre-irradiation drying) may result in a much higher rate of radiolytic H_2 generation, while lower elevated temperatures (100°C) did not produce yields significantly different than at ~30°C; this was speculated to be linked to some degree of thermal dehydration of the bayerite (the 200°C also resulted in ~10% mass loss from the sample) [23].

5.0 Conclusions

Aluminum (oxy)hydroxides and physisorbed water on the surface of aluminum-clad spent nuclear fuel (ASNF) is expected to be a significant source of radiolytic H_2 in ASNF dry storage. Mini-canister experiments described herein measured radiolytic H_2 generation from samples of aluminum alloys with adherent (oxy)hydroxide films in a canister-analogous environment, i.e., a stainless-steel canister with (dry) helium backfill. Three drying processes applied during preparation of the mini-canisters were tested relative to an air-dried condition on four surrogate samples bearing bayerite films, and data was also collected from an air-dried fuel cropping featuring service-formed (oxy)hydroxides. In all cases, the H_2 yields were highest in the low-dose range and tended to decrease with increasing dose, consistent with previous radiolysis data on similar sample types. None of the mini-canister tests displayed an unambiguous plateau indicating net H_2 generation had ceased within the dose range tested, only lower generation rates. No O_2 generation was observed.

The mini-canister results showed a large reduction in radiolytic H_2 yield after heated drying steps (at 150°C or 220°C) compared to an air-dried sample, with little difference between the two temperatures; this reduction in yield is believed to correspond largely to removal of physisorbed water, since the lower drying temperature (150°C) was not expected to decompose bayerite. This impact of heated drying was generally consistent with previous SRNL measurements from samples tested in glass ampoules. The total cumulative H_2 yield from a sample dried by unheated vacuum was closer than expected to that of the air-dried sample, given previous SRNL glass-ampoule data showing substantial reductions in H_2 yield for vacuum-dried compared to air-dried samples. The total yield from the vacuum-dried mini-canister sample increased more rapidly than that of the air-dried sample in the very low-dose range and was only moderately below (~85% of) the air-dried yield by its 1.5 MGy maximum dose. The vacuum-dried sample did have slightly higher bayerite formation, as evidenced by its corrosion mass gain, and the gap between the two samples was larger when normalized by oxide mass: the yield per unit bayerite mass at 1.5 MGy for the vacuum-dried sample was only 66% of the air-dried yield. However, the vacuum-dried yield was much larger over its entire dose range than that of the 150°C or 220°C-dried samples.

The MURR fuel cropping with service-formed (oxy)hydroxides was much smaller than the surrogate samples with a consequently low total yield. However, its yield per unit sample mass was approximately two-thirds that of the air-dried surrogate and roughly three times that of the surrogates subjected to heated drying.

Additionally, elevated concentration of H_2 in the cover gas from an external source (13 vol% H_2) did not appear to have any inhibiting effect on the subsequent H_2 generation, indicating that the rising H_2 concentration is not the cause of the decreasing generation rate, and heat treatments of the two heated-drying canisters up to 200°C after irradiation did not reveal any evidence of additional trapped H_2 or O_2 releasable by heating.

6.0 Future Work

Preparations are underway for a monitored ASNF dry storage pilot using High Flux Isotope Reactor (HFIR) fuel at the Savannah River Site (SRS) [1], which will provide verification and validation data for the drying and safe dry storage of actual ASNF at full-canister scale. The pilot will include two canisters dried by different industrial drying processes, one by vacuum drying and the other by forced-helium dehydration (FHD) under conditions chosen to bring the fuel to at least 220°C and will use intermittent gas sampling similar to that done in the mini-canister testing. The resulting data will confirm whether the difference between vacuum and (220°C) FHD parallels that observed between the unheated vacuum and heated drying conditions in the mini-canister and will also be compared to the predictions of computational models developed by INL based on laboratory data.

In the intervening time, targeted additional radiolysis experiments have been proposed to facilitate preliminary validation stages for the computational model in order to identify and correct any remaining gaps in the modeling of the physical mechanisms prior to scaling up to the full-scale pilot canister. The anticipated experiments would include vacuum-dried tests on 1) a bayerite-bearing surrogate replicating and extending the As-Corroded Vacuum-Only data set up to 15 MGy and 2) a surrogate with mixed-oxide film aiming to more closely replicate the oxide identified during post-irradiation examination of a HFIR inner fuel element. Eventual evaluation of the full set of accumulated radiolysis data (data collected to date from both SRNL and INL as well as the future experiments described above) to attempt to clarify the cause of remaining apparent discrepancies in behavior between different experimental campaigns would also help to refine the model to eliminate gaps prior to full-scale validation.

7.0 References

[1] A. L. d'Entremont, L. N. Ward, R. L. Sindelar, 2023, "ASNF Dry Storage Pilot with HFIR Fuel: Concept Plan," Savannah River National Laboratory, SRNL-STI-2023-00490.

[2] A. d'Entremont, C. G. Verst, B. C. Randall, J. D. McNamara, A. J. Duncan, R. L. Sindelar, 2022, "Radiolysis Testing of SNF Materials and Surrogates in a 'Mini-Canister,'" *Proceedings of Waste Management Symposia 2022*, #22162.

[3] C. G. Verst, A. L. d'Entremont, 2021, "Measurement of Radiolytic Hydrogen Generation and Impact of Drying Treatments on Reactor-Exposed and Surrogate Aluminum Materials," Savannah River National Laboratory, SRNL-STI-2021-00625.

[4] C. Verst, 2022, "Mini-Canister Radiolysis Results – Preliminary Results of Alternate Drying Recipe," Savannah River National Laboratory, SRNL-L3110-2022-00004, Rev. 1.

[5] C. Verst, 2023, "FY2023 Mini-Canister Results," Savannah River National Laboratory, SRNL-L3110-2023-00019.

[6] L. Olson, C. Verst, A. d'Entremont, R. Fuentes, R. Sindelar, 2019, "Characterization of Oxide Films on Aluminum Materials following Reactor Exposure and Wet Storage in the SRS L-Basin," Savannah River National Laboratory, SRNL-STI-2019-00058.

[7] R. S. Wittman, 2013, "Radiolysis Model Sensitivity Analysis for a Used Fuel Storage Canister", Pacific Northwest National Laboratory, FCRD-UFD-2013-000357, PNNL-22773.

[8] A. L. d'Entremont, R. L. Kesterson, R. L. Sindelar, 2020, "Evaluation of Hydrogen Generation in High Burnup Demonstration Dry Storage Cask," Savannah River National Laboratory, SRNL-STI-2020-00268.

[9] G. P. Horne, E. H. Parker-Quaife, C. G. Verst, C. L. Crawford, R. L. Sindelar, 2020, "Milestone 2.6: Complete Round-Robin Hydrogen Gas Analysis Capability Comparison," Idaho National Laboratory, INL/EXT-20-00810, Rev. 1.

[10] C. Verst, B. Randall, J. McNamara, 2020, "Initiate Irradiation and Measurement of Dried Hydrated Oxide Specimens (Large Coupons)," Savannah River National Laboratory, SRNL-L6000-2020-00046.

[11] J. D. McNamara, B. C. Randall, D. J. Pak, A. J. Duncan, A. S. McNight, H. T. Sessions, T. A. Baldwin, D. B. Hunter, 2019, "Status Update on the Instrumented Lid Project," Savannah River National Laboratory, SRNL-L2240-2019-00007.

[12] A. L. d'Entremont, R. E. Fuentes, M. G. Shalloo, T. W. Knight, R. L. Sindelar, 2020, "Thermal Dehydration of Aluminum (Oxy)hydroxides on Fuel Cladding Material," Proceedings of Waste Management Symposia 2020, #20200.

[13] K. Wefers, C. Misra, 1987, "Oxides and hydroxides of aluminum," Alcoa Technical Paper #19, Alcoa Laboratories Pittsburgh, PA.

[14] J. W. Newsome, H. W. Heiser, A. S. Russell, and H. C. Stumpf, 1960, "ALUMINA PROPERTIES. Technical Paper No. 10, Second Revision," Aluminum Co. of America. Alcoa Research Labs., New Kensington, Penna.

[15] J. K. Conrad, G. P. Horne, 2023, "Milestone 1.2.12: The Fate Of Oxygen Radical Species In Corroded Aluminum Alloys Under Irradiation," Idaho National Laboratory, INL/RPT-23-71706.

[16] J. A. Kaddissy, S. Esnouf, D. Durand, D. Saffre, E. Foy, J.-P. Renault, 2017, "Radiolytic Events in Nanostructured Aluminum Hydroxides," *The Journal of Physical Chemistry C* 121, pp. 6365-6373.

[17] C. D. Pilgrim, J. K. Conrad, J. R. Wilbanks, R. P. Morco, J. W. Jones, T. S. Yoder, R. E. Smith, G. P. Horne, "Milestone 1.2.11: H_2 Production from Surrogate Non-Native Corrosion Plumes on Aluminum 6061-T6 Fuel Cladding Surrogates," Idaho National Laboratory, INL/RPT-22-69323.

[18] N. G. Petrik, A. B. Alexandrov, A. I. Vall, 2001, "Interfacial Energy Transfer during Gamma Radiolysis of Water on the Surface of ZrO_2 and Some Other Oxides," *J. Phys. Chem. B* 105, pp. 5935-5944.

[19] A. L. d'Entremont, R. Smith, 2022, "ASNF Drying Recipe - Review of Data," Savannah River National Laboratory, SRNL-L3110-2022-00006.

[20] E. Eidelpes, G. Petersen, 2023, "Bounding Pressure and Flammability Evaluations for a Department of Energy Standard Canister Loaded with Aluminum-Clad Spent Fuel," Idaho National Laboratory, INL/RPT-22-68212, Rev. 2.

[21] A. d'Entremont, R. Smith, C. Rirschl, K. Waldrop, D. Dunn, R. Einziger, R. Sindelar, 2023, "Drying of Spent Nuclear Fuel: Considerations and Examples," *Nuclear Technology* 210(9), pp. 1639–1647. https://doi.org/10.1080/00295450.2023.2226519.

[22] G. P. Horne, J. K. Conrad, T. M. Copeland-Johnson, X. Pu, A. Khanolkar, J. R. Wilbanks, C. D. Pilgrim, 2022, "Milestone 1.2.10: Steady-state H_2 'roll over' point data for aluminum alloys 1100 and 6061," Idaho National Laboratory, INL/RPT-22-68379.

[23] E. H. Parker-Quaife, G. P. Horne, C. R. Heathman, C. Verst, P. R. Zalupski, 2019, "Radiation-Induced Molecular Hydrogen Gas Generation by Pre-Corroded Aluminum Alloy 1100," Idaho National Laboratory, INL/EXT-19-55202, Rev. 1.

[24] G. P. Horne, J. K. Conrad, R. M. Copeland-Johnson, A. Khanolkar, C. D. Pilgrim, J. R. Wilbanks, C. Rae, E. H. Parker-Quaife, 2021, "Milestone 1.2.9: Radiolytic Gas Generation Measurements from Helium-Backfilled Samples of AA1100 and AA6061 Coupons," Idaho National Laboratory, INL/EXT-21-65356.

[25] R. L. Kesterson, R. L. Sindelar, C. G. Verst, G. P. Horne, E. H. Parker-Quaife, 2020, "Evaluation of Radiolysis Data for Hydrogen Gas Generation During Gamma Irradiation of Pre-Corroded and Pristine Aluminum Samples – An Aluminum SNF Dry Storage Study Interim Report," Savannah River National Laboratory, SRNL-STI-2020-00147..

Appendix A. Data tables

Table 7-1: Widths of the 17 mini-canister assembly plates. All plates were 7.000 inches tall and 0.050 inches thick.

Plate number	Width (in)	Width (cm)
1	1.900	4.826
2	2.147	5.453
3	2.340	5.944
4	2.490	6.325
5	2.603	6.612
6	2.692	6.838
7	2.751	6.988
8	2.791	7.089
9	2.763	7.018
10	2.723	6.916
11	2.654	6.741
12	2.544	6.462
13	2.423	6.154
14	2.239	5.687
15	2.024	5.141
16	1.757	4.463
17	1.403	3.564

Table 7-2: Radiolytic yield data for As-Corroded Vacuum-Only surrogate assembly before H_2 spike (Figure 3-6–Figure 3-7) and after restarting the test post-H_2 spike (Figure 3-8).

Dose (MGy)	Gas pressure (kPa)	H_2 gas fraction (%)	Cum. H_2 yield (µmol)	Yield per unit sample mass (µmol/g)	Yield per unit bayerite mass (µmol/g)
0.00	162.4	0.000%	0	0	0
0.02	159.4	0.030%	9.96	0.016	1.18
0.05	156.3	0.055%	18.2	0.029	2.16
0.11	152.8	0.106%	34.2	0.055	4.07
0.17	150.0	0.152%	48.7	0.079	5.79
0.23	147.6	0.181%	58.0	0.094	6.89
0.29	143.4	0.221%	69.4	0.112	8.24
0.35	140.4	0.256%	79.5	0.129	9.45
0.41	138.0	0.303%	93.5	0.152	11.11
0.53	135.7	0.363%	110.5	0.179	13.13
0.63	130.2	0.415%	122.6	0.199	14.58
0.79	126.0	0.472%	136.4	0.221	16.21
0.99	124.6	0.588%	167.5	0.272	19.92
1.45	122.7	0.790%	220.1	0.357	26.16
Post-H_2-spike data					
Dose (MGy)	**Gas pressure (kPa)**	**H_2 gas fraction (%)**	**Cum. H_2 yield (umol)**	**Yield per unit sample mass (µmol/g)**	**Yield per unit bayerite mass (µmol/g)**
0	117.6	13.145%	0	0	0
0.21	118.2	13.196%	31.3	0.051	3.73
0.92	117.1	14.606%	203.8	0.330	24.23
0.92	110.9	14.779%	201.2	0.326	23.92

Table 7-3: Radiolytic yield data for 220°C As-Dried surrogate assembly (Figure 3-6–Figure 3-7).

Dose (MGy)	Gas pressure (kPa)	H_2 gas fraction (%)	Cum. H_2 yield (µmol)	Yield per unit sample mass (µmol/g)	Yield per unit bayerite mass (µmol/g)
0.00	168.6	0.000%	0	0	0
0.03	165.0	0.000%	0	0	0
0.05	161.5	0.000%	0	0	0
0.11	157.1	0.027%	8.8	0.014	1.09
0.18	153.8	0.038%	12.4	0.020	1.53
0.24	150.7	0.048%	15.6	0.025	1.92
0.36	148.1	0.067%	21.5	0.035	2.65
0.46	145.1	0.080%	25.5	0.041	3.15
0.61	140.4	0.100%	30.9	0.050	3.82
0.81	137.6	0.135%	41.0	0.066	5.06
1.21	135.8	0.189%	56.6	0.092	6.99
1.69	132.6	0.221%	65.2	0.106	8.05
1.78	129.1	0.227%	66.5	0.108	8.20
1.84	127.4	0.235%	68.9	0.112	8.50
4.87	95.84	0.749%	182.5	0.296	22.52
5.90	93.29	0.965%	223.5	0.362	27.57
6.93	98.27	1.052%	255.1	0.414	31.47
6.93	85.98	1.059%	233.8	0.379	28.84
7.43	84.12	1.103%	241.1	0.391	29.75
9.51	84.12	1.291%	278.0	0.451	34.30
11.6	82.05	1.254%	270.7	0.439	33.40
15.6	79.43	1.423%	296.1	0.480	36.53

Table 7-4: Radiolytic yield data for 150°C As-Dried surrogate assembly (Figure 3-6–Figure 3-7).

Dose (MGy)	Gas pressure (kPa)	H_2 gas fraction (%)	Cum. H_2 yield (µmol)	Yield per unit sample mass (µmol/g)	Yield per unit bayerite mass (µmol/g)
1.07	172.4	0.167%	59.2	0.092	8.99
2.21	161.3	0.284%	95.1	0.149	14.46
3.42	157.3	0.371%	127.6	0.199	19.40
6.01	157.9	0.544%	186.5	0.291	28.36
9.47	152.3	0.639%	213.5	0.333	32.46
10.7	149.3	0.702%	232.8	0.364	35.40
15.6	143.3	0.756%	244.6	0.382	37.19

Table 7-5: Radiolytic yield data for As-Corroded No-Vacuum surrogate assembly (Figure 3-6– Figure 3-7).

Dose (MGy)	Gas pressure (kPa)	H_2 gas fraction (%)	Cum. H_2 yield (µmol)	Yield per unit sample mass (µmol/g)	Yield per unit bayerite mass (µmol/g)
0.53	183.9	0.188%	70.82	0.111	10.77
1.52	180.3	0.618%	261.21	0.410	39.72
2.52	177.3	1.008%	403.63	0.633	61.38
3.51	174.0	1.353%	525.69	0.825	79.94
4.94	170.2	1.824%	688.34	1.080	104.67
5.92	165.0	2.178%	802.56	1.259	122.04
6.90	162.4	2.375%	879.44	1.380	133.73
8.29	154.6	2.689%	953.09	1.495	144.92
9.12	150.0	2.939%	1045.27	1.640	158.94
10.1	147.5	3.035%	1086.42	1.704	165.20
11.8	144.1	3.415%	1192.50	1.871	181.33
13.6	142.0	3.764%	1302.51	2.043	198.06
14.6	137.6	4.091%	1376.97	2.160	209.38
15.6	136.8	4.306%	1466.50	2.301	222.99

Table 7-6: Radiolytic yield data for MURR cropping sample (Figure 3-6–Figure 3-7).

Dose (MGy)	Gas pressure (kPa)	H_2 gas fraction (%)	Cum. H_2 yield (µmol)	Yield per unit sample mass (µmol/g)
0.00	175.3	0.000%	0	0
0.03	173.0	0.000%	0	0
0.15	170.7	0.000%	0	0
0.31	162.4	0.030%	13.2	0.078
0.42	159.8	0.039%	17.3	0.102
0.51	155.6	0.043%	18.8	0.111
0.56	155.1	0.045%	20.0	0.119
1.69	150.4	0.118%	49.8	0.295
1.87	129.8	0.144%	53.4	0.316
2.06	124.4	0.151%	54.8	0.324
2.33	123.1	0.155%	56.8	0.336
8.05	124.6	0.471%	165.9	0.982
9.12	122.5	0.498%	175.7	1.040
10.2	121.1	0.566%	199.7	1.183
12.0	117.9	0.653%	227.0	1.344
12.9	116.6	0.690%	240.9	1.426
13.8	113.3	0.687%	238.6	1.413
14.8	112.4	0.697%	244.6	1.448
15.7	107.9	0.746%	255.2	1.511
15.7	101.1	0.765%	251.0	1.486